5 GHz A1 Mode Lateral Overtone Bulk Acoustic Resonators in Thin-Film Lithium Niobate

Ruochen Lu, Yansong Yang, and Songbin Gong Department of Electrical and Computer Engineering University of Illinois at Urbana-Champaign, Urbana, IL rlu10, yyang165, songbin@illinois.edu

Abstract— This work presents the first demonstration of the first-order antisymmetric (A1) mode lateral overtone bulk acoustic resonators (LOBAR) in thin-film lithium niobate (LiNbO₃). Thanks to the fast phase velocity, large coupling, and low loss of A1 in LiNbO₃, equally spaced tones around 5 GHz are achieved using a large feature size of 500 nm. Electromechanical coupling (k^2) around 0.4% and high Q over 1000 are observed in more than 20 tones, surpassing the reported overtone resonators at 5 GHz. Meanwhile, the highest Q of 2725, and the highest $f\cdot Q$ product of 1.4·10¹³ are measured at 5.16 GHz. Upon further optimizations, A1 LOBARs can facilitate novel 5G signal processing functions.

Keywords— first-order antisymmetric mode, lateral overtone bulk acoustic resonator, lithium niobate, microelectromechanical systems, piezoelectric resonator

I. INTRODUCTION

In the past decade, the development of radio frequency (RF) microsystems are calling for miniature acoustic elements capable of multi-frequency operations [1]. Different from conventional acoustic resonators, where the piezoelectric transducers and acoustic boundaries are optimized for exciting a specific vibrational mode [2], overmoded resonators are a group of devices designed to efficiently harness a series of equally-spaced resonances within a single resonant body [3]-[5]. Such unique performance can significantly reduce the number of acoustic elements, leading to the miniaturization and simplification of multifrequency acoustic microsystems. In the past few years, various novel RF acoustic signal processing functions have been demonstrated with overmoded resonators, including comb filters [6]-[8], reconfigurable oscillators [9], [10], quantum acoustic systems [11], [12], and integrated soliton microcomb controllers [13]. Upon further advancement of overmoded resonators, more novel functions can be expected.

Among different types of overmoded devices, lateral overtone bulk acoustic resonators (LOBARs) utilize lithographically defined lateral features to generate the overmoded performance [4]. More specifically, the piezoelectric transducers only cover a small section of the resonant cavity, and the higher-order harmonics of the structure are selectively excited, determined by the transducer design [6]. Because of the reduced metal coverage ratio, LOBARs generally feature a high quality factor (Q) for each tone, at the cost of a reduced electromechanical coupling (k^2) from the maximum achievable value in the piezoelectric platforms [14]. Therefore, a high k^2 and low loss RF acoustic platform is sought after for efficient operation at each tone in LOBARs. Recently, LOBARs in thin-film lithium niobate

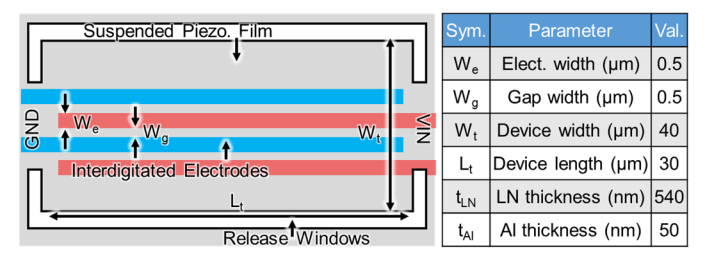


Fig. 1. Mockup of an A1 LOBAR on suspended LiNbO₃ thin film. The key parameters are listed.

(LiNbO₃) have been demonstrated using fundamental shear horizontal (SH0) mode [6], [9]. Thanks to the large k^2 and low loss of SH0 waves in transferred single-crystal LiNbO₃ [15]–[17], LiNbO₃ LOBARs have shown record-breaking k^2 and figure-of-merit (FoM, k^2 ·Q) for various tones, enabling high-performance comb filters [6] and reconfigurable oscillators [10] in the sub-GHz frequency range. However, the slow phase velocity of SH0 (4000 m/s) hurdles the frequency scaling of LOBARs for 5G applications. If directly scaled, a lithography feature size less than 200 nm is required for 5 GHz operation, causing severe electrical loading and fabrication challenges. Thus, a new acoustic platform is needed to scale the LOBAR technologies for high-frequency applications.

To this end, the first-order antisymmetric (A1) mode in LiNbO₃ is a promising candidate. Different from SH0, the operating frequency of A1, as a two-dimensional (2D) mode, can leverage the thickness dimension of LiNbO₃ for scaling up the operating frequency without dramatically reducing the lithography feature size [18]. Thanks to the fast phase velocity and large k^2 (40%), various low-loss, wideband A1 devices have been demonstrated [18]-[24]. However, it is not trivial to design A1 LOBARs. A1 waves tend to be confined within the metalized section of the resonator, suffering from the cut-off of A1 [18], which prohibits the excitation of higher-order overtones in the resonant cavity. This work focuses on the first demonstration of A1 LOBARs. The transducers and acoustic boundaries of A1 LOBARs are first studied to manage the dispersion of A1. The fabricated device shows equally-spaced tones at 5 GHz, using a large feature size of 500 nm. k^2 around 0.4% and high Q over 1000 are observed in more than 20 tones. Meanwhile, the highest Q of 2725 and $f \cdot Q$ product of 1.4·10¹³ are measured at 5.16 GHz. Upon further optimization, the A1 LOBAR can be an essential high-frequency overmoded resonator platform.

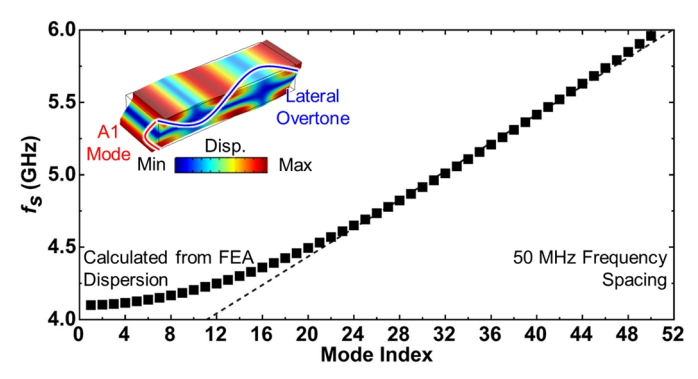


Fig. 2. Calculated resonant frequency of higher-order A1 overtones based on FEA dispersion curves. The displacement mode shape of A1 is plotted.

II. DESIGN AND SIMULATION

The schematic of an A1 LOBAR is presented in Fig. 1 with the key parameters listed in the inset table. The LOBAR is composed of 50 nm aluminum interdigitated transducers (IDTs) on a suspended 540 nm 128° Y-cut LiNbO₃ thin film. The thickness of the thin film is selected for enabling 5 GHz operation using a large feature size of 500 nm [18]. The orientation is selected for maximizing the k^2 of A1 [20]. The release windows are placed on the side for confining the acoustic cavity. For the overmoded operation, only two pairs of IDTs are placed in the center of the resonant body, alternatingly connected to the signal and ground. In operation, a group of higher-order A1 overtones can be supported in the cavity, and the ones matching the periodicity of the IDTs are efficiently excited, forming a typical LOBAR response [9]. The lateral mode order is determined by the number of displacement nodes (2nd order for the example in Fig. 2). Notably, a critical difference between A1 devices and their SH0 counterparts is that both the lateral and thickness dimensions collectively determine the resonant frequencies of A1 modes. It can be approximated through the quasi-static approximation as [18]:

$$f = \sqrt{v_l^2/\lambda^2 + v_t^2/(2t_{LN})^2}$$
 (1)

where f is the operating frequency, v_l is the longitudinal velocity, λ is the lateral wavelength, v_t is the thickness-shear velocity, t_{LN} is the LiNbO₃ film thickness. For A1 waves propagating in 128° Y-cut LiNbO₃ along the material X-axis, v_l and v_t can be approximated by 7000 m/s and 4000 m/s [18]. Following Eq. 1, one can find that a large λ of 2 μ m (i.e., a feature size of 500 nm for IDTs) can enable 5 GHz operation, thanks to the term contributed by the thin-film thickness (t_{LN} = 540 nm). By leveraging A1, one can significantly reduce the feature size requirement by 2.5 times, comparing to SH0 counterparts.

To further capture the dispersion of A1 without the quasistatic approximation, COMSOL finite element analysis (FEA) is performed for an unmetalized cavity with a t_{LN} of 540 nm and a device width (W_t) of 40 µm (Fig. 2). The cut-off can be observed in lower-order A1 modes at 4.1 GHz [18], as predicted by Eq. 1. Higher-order lateral overtones show increasing operating frequencies due to the reduced λ . Moreover, one can notice a region with a nearly linear frequency spacing of 50 MHz around 40^{th} order mode (λ of 2 µm) at 5.3 GHz. The linear fitting is plotted in Fig. 2. It shows that we can achieve 5 GHz equally spaced overtone resonators by matching the periodicity of the IDTs to the λ of 2 µm.

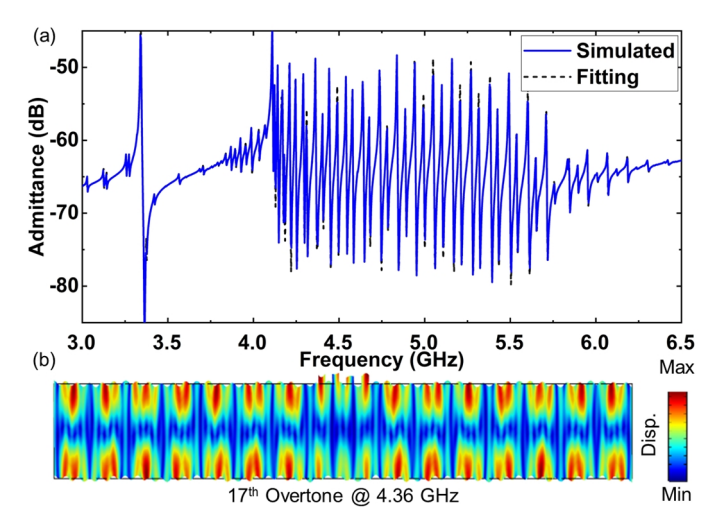


Fig. 3. (a) Simulated admittance response and its fitting using the multi-resonance MBVD model. (b) Mode shape of the 17th overtone at 4.36 GHz.

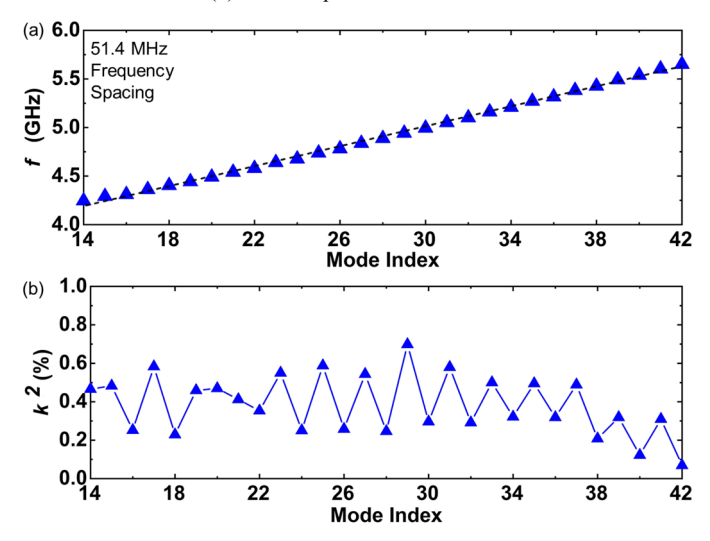


Fig. 4. Extracted key parameters from the simulated admittance, including (a) resonant frequency and (b) k^2 .

To further include the effects of the IDTs, frequency domain FEA is performed for the A1 LOBAR prototype (dimensions listed in Fig. 1). 2D FEA is performed, and the transverse effects are not included. The mechanical Q is set as 1000 since the loss mechanism of A1 in thin-film LiNbO3 is still under research [18]. The admittance response is plotted in Fig. 3 (a). The performance is similar to that of SH0 LOBARs [9], but the resonances are at much higher frequencies around 5 GHz. The displacement mode shape of the 17^{th} A1 lateral overtone at 4.36 GHz is presented in Fig. 3 (b). Note that the LOBAR operates significantly above the cut-off frequency (the mode at 3.3 GHz), and A1 waves can propagate freely into the acoustic cavity [18], which is the critical difference of A1 LOBARs from the previously reported single-mode A1 resonators operating near the cut-off [19]–[23].

The key resonator parameters are then extracted with the recursive multi-resonance MBVD model [25]. The fitting curve is plotted in Fig. 3 (a) and the extracted resonant frequency f and k^2 are listed in Fig. 4. As predicted by the simplified calculation, a frequency spacing of 51.4 MHz is achieved for more than 20

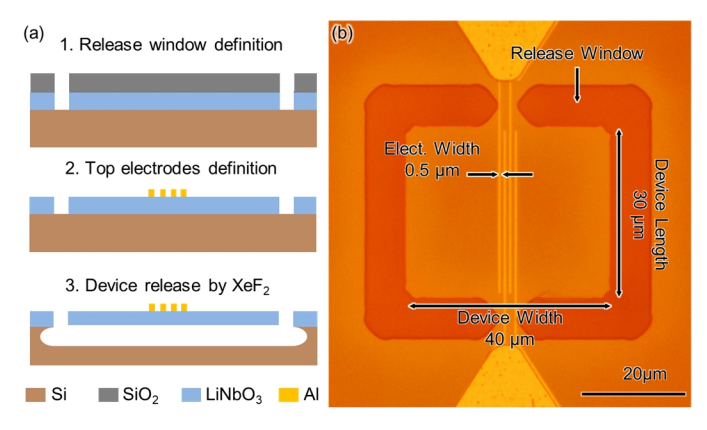


Fig. 5. (a) Fabrication process and (b) optical microscope image of the implemented A1 LOBAR.

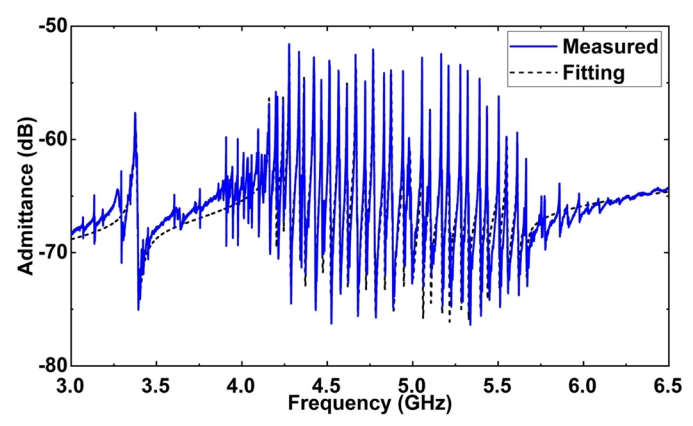


Fig. 6. Measured admittance response and its fitting using the multi-resonance MBVD model.

modes. k^2 around 0.4% is also achieved, even though the IDTs only cover a small portion of the acoustic cavity, thanks to the high intrinsic coupling of A1 in 128° Y-cut LiNbO₃. Some fluctuations of k^2 can be observed in the adjacent modes, due to the slight mode distortion caused by the IDTs. Such results show that the A1 LOBAR in thin-film LiNbO₃ can be an effective platform for implementing efficient overtone resonators for RF acoustic applications above 5 GHz.

III. FABRICATION AND MEASUREMENT

The device is in-house fabricated following the process in [32]. The 540 nm 128° Y-cut LiNbO₃ thin film on a 4-inch silicon (Si) wafer is provided by NGK Insulators, Ltd., for the fabrication [Fig. 5 (a)]. The optical image of the implemented LOBAR is shown in Fig. 5 (b). The acoustic boundaries on the side and the 500 nm wide IDTs are well defined.

The implemented A1 LOBAR is measured with a vector network analyzer (VNA) at the -10 dBm power level in air. The measured admittance is plotted in Fig. 6, showing an overmoded response at 5 GHz. Similarly, the key resonator parameters are then extracted with the recursive multi-resonance MBVD model [25], and the fitting curve is also plotted in Fig. 6, showing a great match. The extracted f, Q, k^2 , and f-Q products are shown in Fig. 7. A frequency spacing of 53.9 MHz is obtained, close to the calculated and simulated values. Thanks to high coupling and low loss of A1 in LiNbO₃, the fabricated device shows k^2 around 0.4% and high Q over 1000 in more than 20 tones around

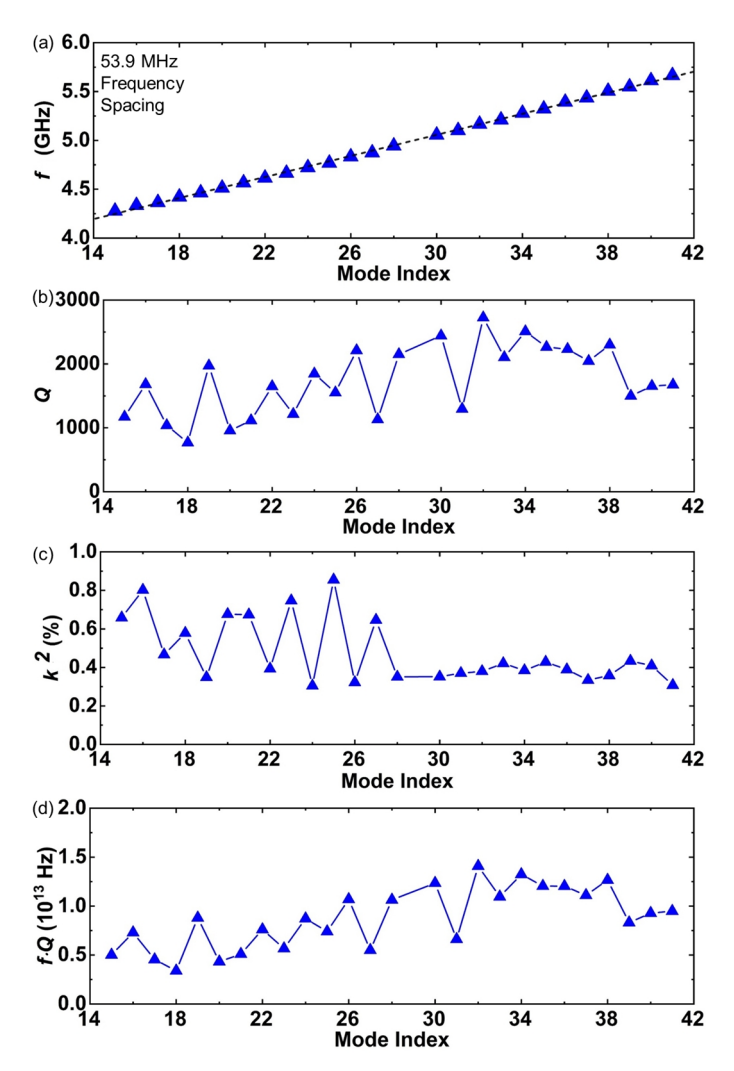


Fig. 7. Extracted key parameters from the measured admittance, including (a) resonant frequency, (b) Q, (c) k^2 , and (d) $f \cdot Q$ products.

5 GHz. The highest Q of 2725 and the highest $f \cdot Q$ product of $1.4 \cdot 10^{13}$ are measured at 5.16 GHz, among the highest reported in piezoelectric resonators at 5 GHz. The fluctuation of k^2 in the is also observed due to the electrical and mechanical loading of the electrodes. Another interesting finding is that the higher frequency tone tends to have a higher Q. Such a result agrees with the theoretical and experimental studies of the propagation loss of A1 waves in thin-film LiNbO₃ [18], [24], [26]. Further loss mechanism studies are needed.

Future studies of A1 LOBARs can be focused on the following aspects. First, the position, thickness, and width of the IDTs should be studied toward a more evenly distribution of k^2 among different modes. Second, the anchor design can be investigated for identifying the loss mechanism and further enhancing Q. Upon further optimization, the A1 LOBARs can lead to an efficient piezoelectric platform for high frequency overmoded applications.

IV. CONCLUSION

In this work, we have demonstrated the first A1 mode LOBAR in thin-film LiNbO₃. The design space is first explored,

and the 5 GHz LOBAR is implemented. Thanks to the fast phase velocity, large k^2 , and low loss of A1 in LiNbO₃, the fabricated device shows k^2 around 0.4% and high Q over 1000 in more than 20 tones around 5 GHz. The highest Q of 2725 and the highest $f \cdot Q$ product of 1.4·1013 are measured at 5.16 GHz, among the highest reported in piezoelectric resonators at 5 GHz. Upon further integrating within the acoustic microsystems, A1 LOBARs, as an essential high frequency, high-performance overmoded resonator platform, can further facilitate various acoustic signal processing functions.

REFERENCES

- [1] J. Tsutsumi, M. Seth, A. S. M. III, R. B. Staszewski, and G. Hueber, "Cost-Efficient, High-Volume Transmission: Advanced Transmission Design and Architecture of Next Generation RF Modems and Front-Ends," *IEEE Microw. Mag.*, vol. 16, no. 7, pp. 26–45, 2015.
- [2] H. Bhugra and G. Piazza, *Piezoelectric MEMS Resonators and Filters*. Springer International Publishing, 2017.
- [3] W. Pang, H. Zhang, J. J. Kim, H. Yu, and E. S. Kim, "High Q single-mode high-tone bulk acoustic resonator integrated with surface-micromachined FBAR filter," *IEEE MTT-S Dig.*, 2005.
- [4] S. Gong, N.-K. Kuo, and G. Piazza, "GHz AlN lateral overmoded bulk acoustic wave resonators with af Q of 1.17× 10 13," in Frequency Control and the European Frequency and Time Forum (FCS), 2011 Joint Conference of the IEEE International, May 2011, pp. 1–5.
- [5] M. Pijolat et al., "Large Qxf product for HBAR using Smart Cut™ transfer of LiNbO3 thin layers onto LiNbO3 substrate," in IEEE Int. Ultrason. Symp., 2008, pp. 201–204.
- [6] R. Lu, T. Manzaneque, Y. Yang, J. Zhou, H. Hassanieh, and S. Gong, "RF Filters with Periodic Passbands for Sparse Fourier Transform-based Spectrum Sensing," *J. Microelectromechanical Syst.*, vol. 27, no. 5, pp. 931–944, 2018.
- [7] K. M. Lakin, G. R. Kline, and K. T. McCarron, "High-Q microwave acoustic resonators and filters," *IEEE Trans. Microw. Theory Tech.*, vol. 41, no. 12, pp. 2139–2146, 1993.
- [8] H. Zhang, W. Pang, H. Yu, and E. S. Kim, "High-tone bulk acoustic resonators on sapphire, crystal quartz, fused silica, and silicon substrates," *J. Appl. Phys.*, vol. 99, no. 12, p. 124911, 2006.
- [9] R. Lu, T. Manzaneque, Y. Yang, A. Kourani, and S. Gong, "Lithium Niobate Lateral Overtone Resonators for Low Power Frequency-hopping Applications," in *IEEE 31rd International Conference on Micro Electro Mechanical Systems*, 2018, pp. 751–754.
- [10] A. Kourani, R. Lu, and S. Gong, "A Wideband Oscillator Exploiting Multiple Resonances in Lithium Niobate MEMS Resonator," *IEEE Trans. Ultrason. Ferroelectr. Freq. Control*, vol. 67, no. 9, pp. 1854–1866, 2020.
- [11] V. J. Gokhale, B. P. Downey, D. S. Katzer, L. B. Ruppalt, and D. J.

- Meyer, "GaN-based Periodic High-Q RF Acoustic Resonator with Integrated HEMT," in 2019 IEEE International Electron Devices Meeting (IEDM), 2019, pp. 17.5.1-17.5.4.
- [12] V. J. Gokhale et al., "Epitaxial bulk acoustic wave resonators as highly coherent multi-phonon sources for quantum acoustodynamics," Nat. Commun., vol. 11, no. 1, pp. 1–9, 2020.
- [13] J. Liu et al., "Monolithic piezoelectric control of soliton microcombs," Nature, vol. 583, no. 7816, pp. 385–390, 2020.
- [14] H. Bhugra and G. Piazza, Piezoelectric MEMS Resonators. Springer, 2017.
- [15] R. H. Olsson et al., "A high electromechanical coupling coefficient SH0 Lamb wave lithium niobate micromechanical resonator and a method for fabrication," Sensors Actuators A Phys., vol. 209, pp. 183–190, 2014.
- [16] R. Lu, Y. Yang, M.-H. Li, T. Manzaneque, and S. Gong, "GHz Broadband SH0 Mode Lithium Niobate Acoustic Delay Lines," *IEEE Trans. Ultrason. Ferroelectr. Freq. Control*, vol. 67, no. 2, pp. 402–412, 2020.
- [17] M. Kadota, Y. Kuratani, T. Kimura, M. Esashi, and S. Tanaka, "Ultra-wideband and high frequency resonators using shear horizontal type plate wave in LiNbO3 thin plate," *Jpn. J. Appl. Phys.*, vol. 53, no. 7S, p. 07KD03, 2014.
- [18] R. Lu, Y. Yang, M.-H. Li, and S. Gong, "5-GHz Antisymmetric Mode Acoustic Delay Lines in Lithium Niobate Thin Film," *IEEE Trans. Microw. Theory Tech.*, vol. 68, no. 2, pp. 573–589, 2020.
- [19] Y. Yang, R. Lu, L. Gao, and S. Gong, "4.5 GHz Lithium Niobate MEMS Filters with 10% Fractional Bandwidth for 5G Front-ends," J. Microelectromechanical Syst., vol. 28, no. 4, pp. 575–577, 2019.
- [20] R. Lu, Y. Yang, S. Link, and S. Gong, "A1 Resonators in 128° Y-cut Lithium Niobate with Electromechanical Coupling of 46.4%," J. Microelectromechanical Syst., pp. 1–7, 2020.
- [21] V. Plessky, S. Yandrapalli, P. J. Turner, L. G. Villanueva, J. Koskela, and R. B. Hammond, "5 GHz laterally-excited bulk-wave resonators (XBARs) based on thin platelets of lithium niobate," *Electron. Lett.*, vol. 55, no. 2, pp. 98–100, 2018.
- [22] P. J. Turner et al., "5 GHz Band n79 wideband microacoustic filter using thin lithium niobate membrane," Electron. Lett., vol. 55, no. 17, pp. 942– 944, 2019.
- [23] M. Kadota, T. Ogami, K. Yamamoto, Y. Negoro, and H. Tochishita, "High-frequency Lamb wave device composed of LiNbO3 thin film," *Jpn. J. Appl. Phys.*, vol. 48, no. 7S, p. 07GG08, 2009.
- [24] R. Lu, Y. Yang, S. Link, and S. Gong, "Low-Loss 5 GHz First-Order Antisymmetric Mode Acoustic Delay Lines in Thin-Film Lithium Niobate," *IEEE Trans. Microw. Theory Tech.*, 2020.
- [25] R. Lu, M.-H. Li, Y. Yang, T. Manzaneque, and S. Gong, "Accurate Extraction of Large Electromechanical Coupling in Piezoelectric MEMS Resonators," *J. Microelectromechanical Syst.*, vol. 28, no. 2, pp. 209– 218, 2019.
- [26] V. Plessky, J. Koskela, and S. Yandrapalli, "Attenuation of Lamb modes and SH waves near cut-off frequencies," *IEEE Int. Freq. Control Symp.*, 2020.